Jpn J Ophthalmol (2014) 58:177–187
DOI 10.1007/s10384-013-0297-x

THE OFFICIAL INTERNATIONAL JOURNAL OF THE JAPANESE OPHTHALMOLOGICAL SOCIETY

CLINICAL INVESTIGATION

Two types of acute zonal occult outer retinopathy differentiated by dark- and light-adapted perimetry

Kazuki Kuniyoshi · Hiroyuki Sakuramoto · Yuzo Nakao · Chota Matsumoto · Yoshikazu Shimomura

Received: 27 June 2013 / Accepted: 29 October 2013 / Published online: 26 December 2013

Abstract
Purpose To assess the results of perimetry recorded under dark- and light-adapted (DA and LA) conditions in patients with acute zonal occult outer retinopathy (AZOOR) and to compare the results of electroretinography (ERG) and spectral-domain optical coherence tomography (SD-OCT) in two groups of AZOOR patients.
Methods Twelve patients with AZOOR were studied. The diagnosis of AZOOR was based on the results of ophthalmoscopy, Goldmann kinetic perimetry, and multifocal ERGs. In addition, DA and LA perimetry, ERG, and SD-OCT were performed. The patients were followed for 1–9 years.
Results The patients were classified into two types: type A patients (3) had a scotoma detected by both DA and LA perimetry, normal or equally abnormal cone and rod ERGs, atrophy of the outer nuclear layer (ONL), and disruption of the inner segment/outer segment (IS/OS) junction line in the OCT images. Type B patients (7) had a scotoma that was more prominent in LA than in DA perimetry and a continuous IS/OS junction line in the OCT images. Two patients had characteristics of both type A and type B AZOOR.
Conclusions Our findings suggest that eyes with type A AZOOR have focal and severe impairment of both the rods and cones, and eyes with type B AZOOR have focal and specific impairment of the cones.

Keywords Acute zonal occult outer retinopathy · Perimetry · Dark adaptation · Light adaptation · Electroretinography

Introduction

Acute zonal occult outer retinopathy (AZOOR) is an acquired retinal disorder first reported by Gass in 1993 [1]. The major characteristics of AZOOR are sudden onset of visual field disturbances, photopsia, and decrease in vision [1–16]. Ophthalmoscopy at the onset of the disease shows minimal abnormalities, and the results of electroretinography (ERG) indicate retinal dysfunctions in the area corresponding to the visual field disturbances [1–16]. AZOOR affects healthy 20- to 50-year-old individuals, and the majority of patients have unilateral symptoms at the onset [1–16]. According to Gass, half of AZOOR patients develop retinal degeneration during the follow-up period [3]. The etiology of AZOOR has not been determined, and no effective treatment is known, except for two studies that reported that virucides [15] and corticosteroids [16] were effective.

AZOOR is part of the acute idiopathic blind spot enlargement (AIBSE) syndrome [17] in which the blind spot enlargement is caused by focal retinal dysfunction with subtle abnormal findings of the retina. At present, the AIBSE syndrome includes AZOOR, multiple evanescent white dot syndrome (MEWDS), punctate inner choroidopathy (PIC), and multifocal choroiditis (MFC); these conditions are jointly referred to as the AZOOR complex [17–20].

Electronic supplementary material The online version of this article (doi:10.1007/s10384-013-0297-x) contains supplementary material, which is available to authorized users.

K. Kuniyoshi (✉) · H. Sakuramoto · Y. Nakao · C. Matsumoto · Y. Shimomura
Department of Ophthalmology, Kinki University Faculty of Medicine, 377-2 Ohno-Higashi, Osaka-Sayama, Osaka 589-8511, Japan
e-mail: kazuki@med.kindai.ac.jp

Table 1 Summary of clinical findings of patients with AZOOR

Patient	Age/ sex/ eye at onset	Follow-up years	Treatment	Photopsia		BCVA at the initial	BCVA at the latest	Refractive error	Fundi at the initial	Fundi at the latest	Scotoma shape	Scotoma during follow-up	Scotoma size after light adaptation	ERG of the affected eye	OCT at the scotoma	Note	Type (Table 2)
1	42/F/ OD	7	No	No	**OD**	**1.2**	**1.2**	**−9.25**	**WNL**	**WNL**	**BSE**	**Slightly improved**	**No change**	**Cones: reduced**	**IS/OS disrupted**		**A**
					OS	1.2	1.2	−9.75						**Rods: reduced**	**ONL extinguished**		
2	25/F/ OS	2	No	Yes	OD	1.2	1.2	+0.25	**WNL**	**WNL**	**BSE**	**Enlarged**	**No change**	**Cones: reduced**	**IS/OS disrupted**	CME	**A**
					OS	**1.2**	**1.2**	**+0.25**						**Rods: reduced**	**ONL extinguished**		
3	32/F/ OD	1	Steroids (pulse)	Yes	**OD**	**1.2**	**1.2**	**−13.0**	**WNL**	**WNL**	**BSE**	(NA)	**No change**	**Cones: delayed**	**IS/OS disrupted**		**A**
					OS	1.2	1.2	−12.0						**Rods: normal**	**ONL atrophy**		
4	36/M/ OD	9	No	No	**OD**	**1.0**	**1.0**	**−1.0**	**WNL**	**WNL**	**BSE**	**Improved**	**Enlarged**	**Cones: reduced**	**COST indistinct**		**B**
					OS	1.2	1.0	−1.0						**Rods: normal**	**ONL atrophy**		
5	46/M/ OS	1	No	No	OD	2.0	2.0	+0.25	**WNL**	**WNL**	**BSE**	(NA)	**Enlarged**	**Cones: normal**	(NA)		**B**
					OS	**2.0**	**2.0**	**+0.25**						**Rods: normal**			
6	44/F/ OS	4	Steroids (pulse)	Yes	OD	2.0	1.5	+0.5	**WNL**	**WNL**	**BSE**	(NA)	**Enlarged**	**Cones: reduced**	**Unremarkable**		**B**
					OS	**1.5**	**0.9**	**+0.5**						**Rods: slightly reduced**			
7	26/M/ OD	6	No	No	**OD**	**1.0**	**1.0**	**−5.5**	**WNL**	**WNL**	**BSE**	**Improved**	**Enlarged**	**Cones: reduced**	**Unremarkable**		**B**
					OS	1.0	1.0	−4.0						**Rods: slightly reduced**			
8	26/M/ OS	1	No	No	OD	1.2	1.2	−2.0	**WNL**	**WNL**	**Constriction**	(NA)	**Enlarged**	**Cones: severely reduced**	**Unremarkable** (OCT 3000)		**B**
					OS	**1.5**	**1.5**	**−2.0**						**Rods: normal**			
9	38/F/ OD	1	No	Yes	**OD**	**1.0**	**1.0**	**+0.25**	**WNL**	**WNL**	**Ring-shaped**	(NA)	**Enlarged**	**Cones: reduced**	**Unremarkable**		**B**
					OS	1.0	1.0	+0.25						**Rods: bilaterally reduced**			

Table 1 continued

Patient	Age/ sex/ eye at onset	Follow-up years	Treatment	Photopsia		BCVA at the initial	BCVA at the latest	Refractive error	Fundi at the initial	Fundi at the latest	Scotoma shape	Scotoma during follow-up	Scotoma size after light adaptation	ERG of the affected eye	OCT at the scotoma	Note	Type (Table 2)
10	34/F/ OS	2	No	No	OD	1.2	1.2	−10.0	WNL	WNL	Nasal hemianopia	Improved	Enlarged	Cones: reduced	Unremarkable		B
					OS	**1.2**	**1.2**	**−10.0**						**Rods: slightly reduced**			
11	28/F/ OD	1	No	Yes	**OD**	**1.0**	**1.2**	**−0.5**	WNL	WNL	BSE + Central	No change	Enlarged	Cones: reduced & delayed	COST indistinct		A + B
					OS	1.5	1.5	+0.25						**Rods: slightly reduced**			
12	26/M/ OS	3	Steroids (oral)	No	OD	1.0	1.0	−6.5	Scar	Scar	BSE + Central	Improved	Enlarged	Cones: severely reduced	IS/OS disrupted and ONL extinguished at the fovea	MFC OU	A + B
					OS	**0.5**	**0.4**	**−7.5**	**Scar**	**Scar**				**Rods: reduced**		RD OD	

Boldface: findings of the affected eye

BCVA best-corrected visual acuity, *ERG* electroretinogram, *OCT* optical coherence tomography, *WNL* within normal limits, *BSE* blind spot enlargement, *NA* not available, *IS/OS* inner-/outer-segment junction line, *ONL* outer nuclear layer, *COST* cone outer segment tip line, *CME* cystoid macular edema, *MFC* multifocal choroiditis, *RD* history of retinal detachment surgery

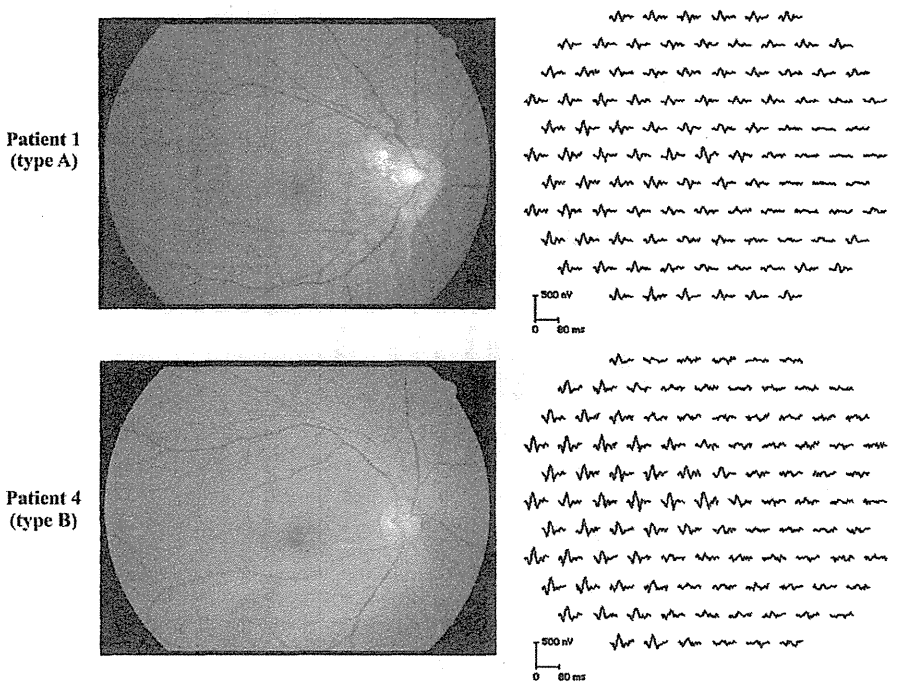

Fig. 1 Fundus photographs and multifocal electroretinograms (*mfERGs*) of the affected eye in patients 1 and 4

High-resolution optical coherence tomography (OCT) and adaptive optics scanning laser ophthalmoscopy (AO-SLO) have been improved, and the newer models have allowed clinicians to investigate the microstructure of the retina in more detail. The OCT images recorded from patients with the AZOOR complex show abnormalities of the outer layers of the retina including the inner segment-outer segment (IS/OS) junction line [6–11, 14, 20] and the cone outer segment tip (COST) line [11, 12]. In 2011, observations of the retina with an AO-SLO suggested a selective loss of cones with relatively well-maintained rods in the area of the scotoma [13, 14].

Dark- and light-adapted (DA and LA) perimetry has been used to study the retinal dysfunction in patients with cone dysfunction syndrome [21–23], retinitis pigmentosa [23, 24], and other retinal disorders [2, 21, 24, 25]. The results of DA and LA perimetry in three patients with AZOOR were reported by our laboratory, and we suggested that there were selective focal impairments of the cones [26, 27].

The purpose of this study was to compare the DA and LA visual fields and OCT images with the clinical features of 12 AZOOR patients.

Patients and methods

The research protocol was approved by the Ethics Review Board of the Kinki University Faculty of Medicine, and the procedures conformed to the tenets of the Declaration of Helsinki. All clinical tests were performed after obtaining signed informed consent from all of the patients.

We studied 12 Japanese patients (5 men and 7 women) who were diagnosed with AZOOR at Kinki University Hospital from July 2003 to June 2013. AZOOR was diagnosed on the basis of the clinical history, ophthalmoscopy, Goldmann kinetic perimetry, and multifocal ERGs (mfERGs). Fluorescein fundus angiography (FA), indocyanine-green fundus angiography (IA), Octopus automated static perimetry, International Society for Clinical Electrophysiology of Vision (ISCEV)-Standard full-field ERG [28], and OCT were also used.

The stimuli for the ISCEV-Standard full-field ERGs [28] were obtained from white light-emitting diodes (LEDs) embedded in a contact-lens electrode (EW-102 and WLS-20; Mayo Corp., Inazawa, Japan). A bioamplifier (MEB-5504; Nihon Kohden, Tokyo, Japan) was used to amplify and record the ERGs. mfERGs were recorded with the Visual Evoked Response Imaging System (Veris Science 5.0; Electro-Diagnostic Imaging, Redwood City, CA, USA).

Three background luminances were used for the kinetic perimetry: 0 cd/m^2 or 0 asb for the DA kinetic perimetry, 10.0 cd/m^2 or 31.5 asb for the conventional kinetic perimetry, and 34 cd/m^2 or 106.8 asb for the LA kinetic perimetry. The DA kinetic perimetry was carried out after 20 min of dark adaptation, and the LA kinetic perimetry after 10 min of light adaptation with a background light of 34 cd/m^2. All kinetic perimetry was performed by a well-trained technician in a light-tight room.

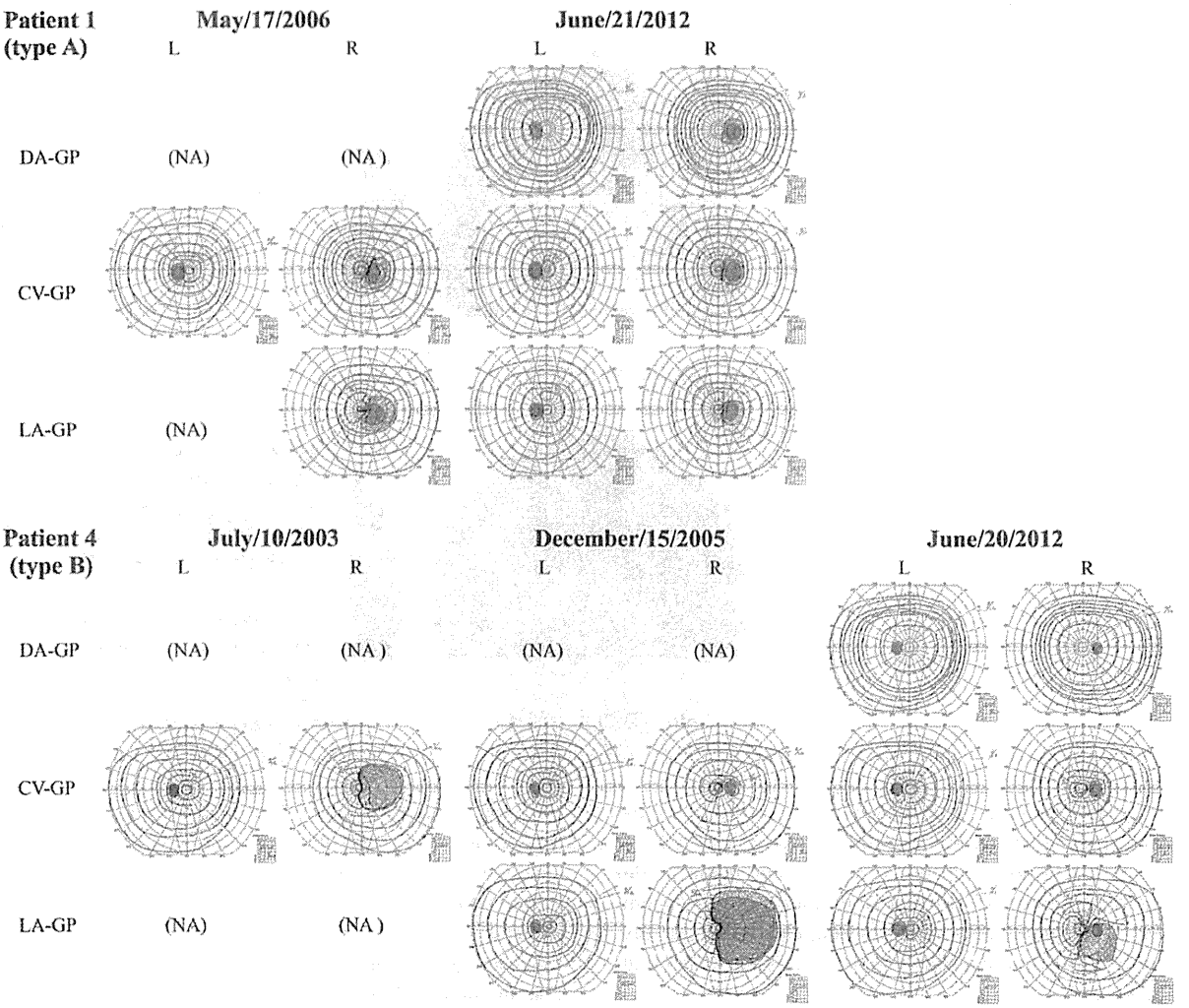

Fig. 2 Results of Goldmann kinetic perimetry (*GP*) in patients 1 and 4. Dark-adapted and light-adapted GPs (*DA-GP* and *LA-GP*) were performed in addition to the conventional GP (*CV-GP*). In patient 4 on 15 December 2005, no scotoma was detected by CV-GP although a large and dense scotoma was detected by LA-GP, and it remained 9 years after the onset. *NA* indicates not available

Static perimetry was performed in three patients (patients 4, 5, 6) using the Octopus 101 automated perimeter (Haag-Streit, Koeniz, Switzerland) under both DA and LA conditions. The DA and LA static perimetry was performed under the same conditions as DA and LA kinetic perimetry, i.e., with no background and with background light of 34 cd/m^2 after LA. Both DA and LA static perimetries were performed using Program 32 with the Normal strategy. The size and duration of the targets were 1 and 100 ms for the DA static perimetry and 3 and 200 ms for the LA static perimetry. A small dim red cross was used as a fixation target for the DA static perimetry and a green cross for the LA static perimetry. The visual fixation was monitored with an infrared camera. A panel located in front of the Octopus 101 automated perimeter was covered with a dark-red plastic plate. The perimeter was light-tight, and no leak from the light source of the perimeter was detected during the examination.

The OCT images were obtained with spectral domain (SD)-OCT (Cirrus^{TM} HD-OCT version 5.1; Carl Zeiss Meditec, Dublin, CA, USA). The five-line scans with a distance of 75 μm between lines were performed, and four images were averaged. The length of the scan was 9.0 mm horizontally and 6.0 mm vertically. The OCT scan was centered on the fovea, and temporal and nasal scans were also performed to cover the area of the scotoma.

Results

The clinical characteristics of the 12 patients with AZOOR are listed in Table 1. All of the patients were generally

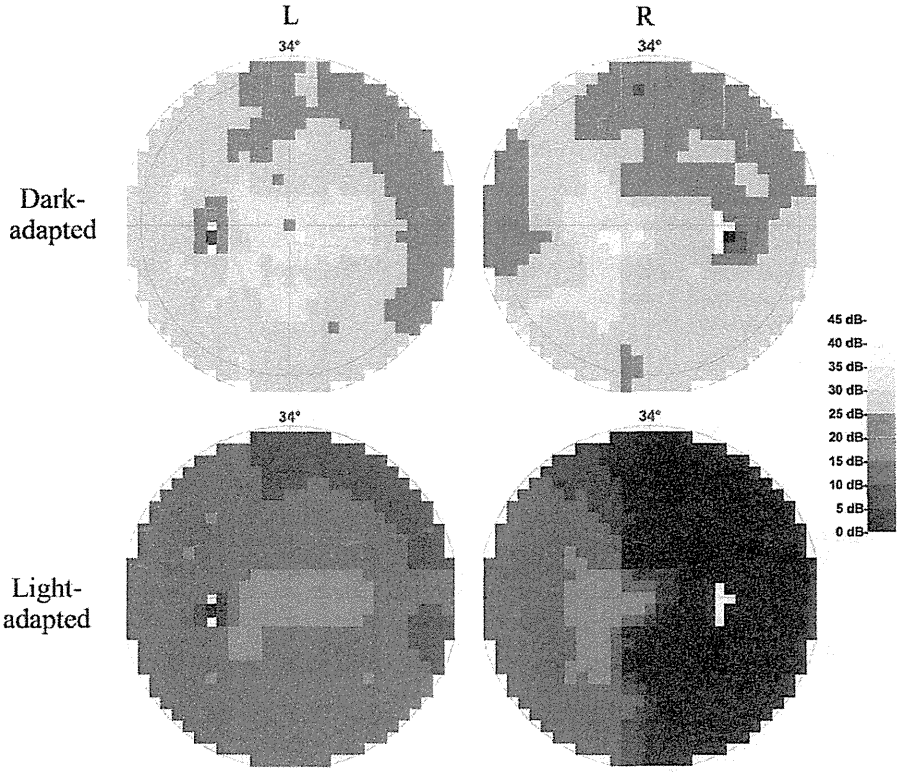

Fig. 3 Results of dark- and light-adapted Octopus automated static perimetry obtained from patient 4 (type B AZOOR). In the *right* eye, sensitivity of the retina was normal on dark-adapted perimetry where a dense scotoma was detected on light-adapted perimetry

healthy, and their age at the onset of the symptoms ranged from 25 to 46 years. The patients were followed for 1–9 years with no medications, except three patients who were treated with corticosteroids by the referring hospital. Because the treatments were ineffective, they were discontinued before the patients were referred to our clinic (Table 1).

At the initial visit, the fundus of all patients appeared normal despite the sudden onset of visual field abnormalities (Fig. 1; Online Resource 1). The visual field abnormalities were unilateral in all of the patients, and reduced mfERGs were detected in the corresponding areas of the visual field abnormalities (Fig. 1; Online Resource 1). Photopsia was reported in 5 of the 12 patients. The vision was normal in all of the patients except in patient 12, in whom a central scotoma developed during the follow-up period (Table 1; Online Resource 5). Twelve eyes of six patients were within ± 1.0 D; six eyes of three patients were myopic with a range of −1.0 to −8.0 D; and six eyes of three patients had myopia >8.0 D (Table 1).

During the follow-up period, the fundus remained normal in all of the patients, even patients 1, 4, 6, and 7, who were followed for more than 3 years (Table 1). FA and IA were unremarkable in all of the patients. FA and IA were not performed for patient 2 because of pregnancy.

The location and shape of the visual field defects were as follows: seven patients with an enlargement of the blind spot (BSE), two patients with a combination of a BSE and a central scotoma, one patient with nasal hemianopia, one patient with overall constriction of the visual field, and one patient with a ring-shaped scotoma (Table 1; Online Resources 2–5).

In patients 1, 2, and 3, the size of the scotoma was the same on both DA and LA perimetry or larger on DA perimetry (Figs. 2, 4; Online Resource 2). On the other hand, in patients 4–10, a deep scotoma was detected by LA perimetry, but not by DA perimetry (Figs. 2, 3, 4; Online Resources 3–5). During the follow-up period, the area of the visual field abnormalities increased in patient 2 and decreased in patients 1, 4, 7, 10, and 12 (Online Resources 2–5). In the ERG tests, both the rod and cone ERGs had normal amplitudes in patients 3 and 5, both the rod and cone ERGs were reduced in the affected eye of patients 1 and 2, and the cone ERGs were more reduced than the rod ERGs in the affected eye of patients 4 and 6–12 (Table 1; Figs. 5, 6; Online Resources 2–5).

In the OCT images, the IS/OS junction line was disrupted, and the ONL was thinner in the area where the scotomas were detected on both DA and LA perimetry in patients 1, 2, 3, and 12 (Fig. 7; Online Resource 6, white bars). The COST line was indistinct in the area where the scotoma was detected on LA perimetry in patients 4 and 11 (Fig. 7 and Online Resource 6, gray and white bars). No abnormal findings were found in the HD-OCT images of

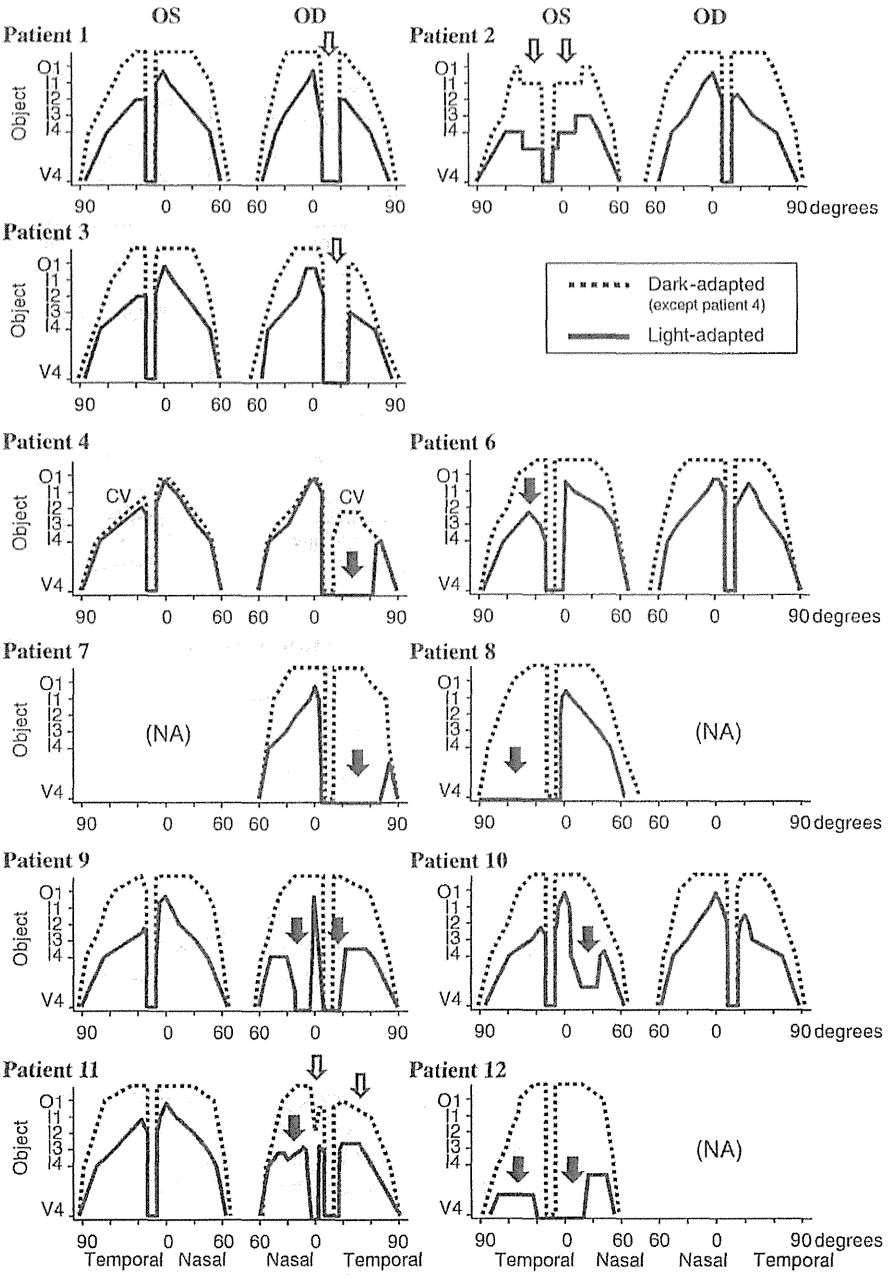

Fig. 4 Horizontal profile of retinal sensitivity measured by DA-GP (*dotted lines*) and LA-GP (*solid lines*). The *open arrows* indicate the scotoma that was detected by both DA- and LA-GP (type A AZOOR), and the *closed arrows* indicate the scotoma that was detected by LA-GP but not by DA-GP (type B AZOOR). In patient 4, conventional GP (CV; *dotted lines*) was performed instead of LA-GP. *NA* indicates not available

patients 6, 7, 9, and 10. Cystoid macular edema was found in patient 2, but the visual acuity was not reduced (Table 1; Online Resource 6).

Discussion

Our results showed that patients with AZOOR can be divided into two types according to the DA and LA perimetric findings: type A patients have scotomas that are detected by both DA and LA perimetry (patients 1, 2, 3; Fig. 2; open arrows in Fig. 4; Online Resource 2), and type B patients have scotomas that are more prominent in LA than in DA perimetry (patients 4–10; Fig. 2; closed arrows in Fig. 4; Online Resources 3–5).

The type A patients (patients 1–3) had normal or reduced cone and rod ERGs, a disrupted IS/OS junction line, and atrophic ONL (Figs. 5, 6, 7; Online Resources 2 and 6). These findings suggest focal atrophy of both the rods and cones (Table 2).

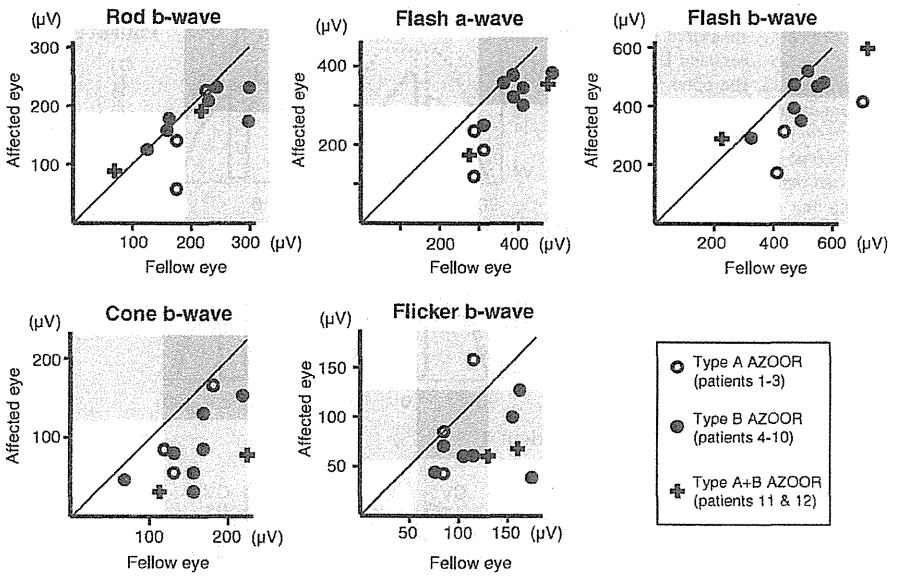

Fig. 5 Amplitudes of the full-field ERGs. The *shaded areas* indicate the normal range

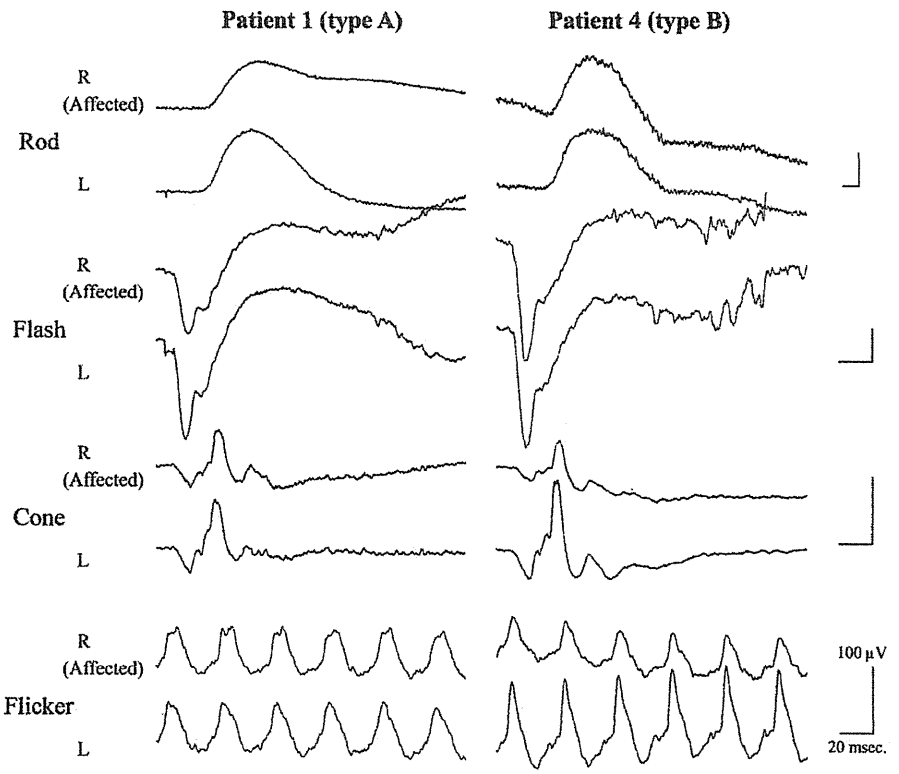

Fig. 6 Results of International Society for Clinical Electrophysiology of Vision (ISCEV)-Standard full-field ERGs in patients 1 and 4. In patient 4 (type B AZOOR), the cone responses including the flicker ERG were reduced in the affected eye, whereas the rod ERG showed the same amplitude in both eyes

On the other hand, type B patients (patients 4–10) had large visual field defects in the LA perimetric fields that were not detected after dark adaptation (Figs. 2, 3; Online Resources 3–5). The retinal sensitivities measured across the horizontal meridian with Goldmann kinetic perimetry are shown in Fig. 4. The results of DA perimetry in patients 4–10 showed normal sensitivity where the scotoma was detected by LA perimetry (Fig. 4, closed arrows). In the type B patients, the cone ERGs were more reduced than the rod ERGs (Figs. 5, 6; Online Resources 3–5). The OCT images of patients with type B AZOOR showed a continuous IS/OS junction line in all patients and ONL thinning

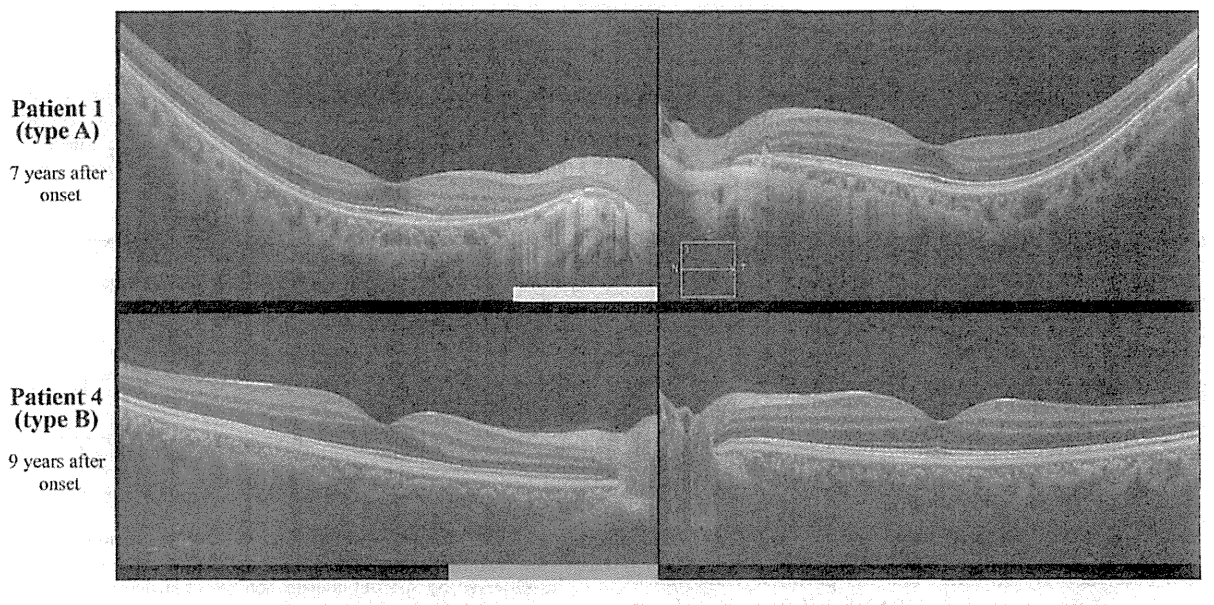

Fig. 7 Results of optical coherence tomography (OCT) with Cirrus^{TM} HD-OCT in patients 1 and 4. The *white and gray bars* beneath the images indicate the corresponding area to the scotoma. In patient 1, the inner segment/outer segment (IS/OS) junction line was disrupted, and the outer nuclear layer (ONL) was atrophic where the scotoma was detected (*white bar*; type A AZOOR), whereas in patient 4, the IS/OS junction line was continuous, the cone outer segment tip (*COST*) line was indistinct, and the ONL was thin but remained where the scotoma was detected by the LA-GP (*gray bar*; type B AZOOR)

Table 2 Characteristics of the two types of AZOOR

	Full-field ERG	Visual field abnormality	OCT findings at the scotoma	Prognosis	Presumed pathogenesis
Type A	Within normal limits or both rod and cone responses reduced	Detectable under both dark- and light-adapted conditions	Atrophic ONL and absence of IS/OS junction line	Stable or deteriorated	Focal photoreceptor dysfunction (atrophy)
Type B	Within normal limits or cone response more reduced than rod response	Prominent under light-adapted conditions and undetectable under dark-adapted conditions	Unremarkable or indistinct COST line and ONL thinning in the long-term	Stable or improved	Focal cone dysfunction

in one of the seven patients (Table 1; Fig. 7; Online Resource 6).

These findings suggest that the retinal impairment in type B AZOOR is milder and less progressive than that in type A AZOOR. In addition, LA perimetry suggested a focal cone dysfunction where the scotoma was detected. These unique findings correspond with those of recent reports on the selective abnormality of the COST line [11, 12] or the selective loss of the cones [13, 14] in AZOOR patients and are similar to the findings of previous case reports [5, 22, 25].

Although some type B AZOOR patients had a reduction of the scotoma during the follow-up period (Table 1; Fig. 2), they complained that the symptoms were not improved. They reported a dense scotoma in a bright room or outdoors on sunny days, but the scotoma disappeared in darkened rooms or outdoors at night. These complaints are consistent with the results of DA and LA perimetry in patients with type B AZOOR and suggest that LA perimetry is more useful than conventional perimetry for detecting visual field abnormalities in type B patients.

The analysis of the scotoma was complicated in patients 11 and 12. In patient 11, a scotoma involving the macular area was detected on both DA and LA perimetry, although the vision was good, and the OCT showed a continuous IS/OS line with an indistinct COST line (Online Resources 5 and 6). Patient 12 showed the characteristics of type B AZOOR at the initial visit; however, a central scotoma appeared during the follow-up period that was detected by both DA and LA perimetry. In addition, the IS/OS junction line at the central scotoma was disrupted in the OCT images (Online Resources 5 and 6). Full-field ERGs recorded in both patients showed a cone-dominant

dysfunction (Online Resource 5), consistent with the characteristics of type B AZOOR.

We concluded that, for the present, these patients are type A + B (Table 1); a final conclusion regarding the AZOOR type will probably be made after future longitudinal clinical observations.

Jacobson et al. [2] examined 24 patients with AZOOR and allied diseases and reported that absolute scotomas were detected by both DA and LA static perimetry. In addition, both rod and cone ERGs were significantly reduced in these eyes. These results indicate that most of the patients in Jacobson et al.'s study [2] had the characteristics of type A AZOOR. Type A AZOOR, which is clinically more severe than type B, may be more prevalent in other countries than in Japan.

In summary, our results indicate that patients with AZOOR can be divided into two types according to the results of DA and LA perimetry, ERGs, and OCT (Table 2).

Patients classified as having type A AZOOR had scotoma detectable by both DA and LA perimetry, and those classified as having type B AZOOR had more prominent scotoma detected better by LA than by DA perimetry. The retinal dysfunction in type A AZOOR is probably due to severe focal photoreceptor atrophy and that in type B AZOOR to focal and cone-specific dysfunction. The prognosis of type A AZOOR appears to be poorer than that of type B AZOOR. Further studies are needed because of the limitation of the number of cases and the length of the follow-up period of this study.

Acknowledgments The authors express gratitude to Kazuyo Nakada-Omure, C.O., Department of Ophthalmology, Kinki University Faculty of Medicine, for her continuous technical assistance, especially for performing the dark- and light-adapted Goldmann kinetic perimetry for this research. This research was supported in part by research grants from the Japanese Ministry of Health, Labor, and Welfare, and from the Japan Society for the Promotion of Science.

Conflicts of interest K. Kuniyoshi, None; H. Sakuramoto, None; Y. Nakao, None; C. Matsumoto, None; Y. Shimomura, None.

References

1. Gass JDM. Acute zonal occult outer retinopathy. J Clin Neuroophthalmol. 1993;13:79–97.
2. Jacobson SG, Morales DS, Sun XK, Feuer WJ, Cideciyan AV, Gass JDM, et al. Pattern of retinal dysfunction in acute zonal occult outer retinopathy. Ophthalmology. 1995;102:1187–98.
3. Gass JD, Agarwal A, Scott IU. Acute zonal occult outer retinopathy: a long-term follow-up study. Am J Ophthalmol. 2002;134:329–39.
4. Arai M, Nao-i N, Sawada A, Hayashida T. Multifocal electroretinogram indicates visual field loss in acute zonal occult outer retinopathy. Am J Ophthalmol. 1998;126:466–9.
5. Machida S, Kizawa J, Fujiwara T, Murai K, Sugawara E, Imaizumi N. Unilateral cone dysfunction as a manifestation of acute zonal occult outer retinopathy. Retin Cases Brief Rep. 2007;1:223–8.
6. Li D, Kishi S. Loss of photoreceptor outer segment in acute zonal occult outer retinopathy. Arch Ophthalmol. 2007;125:1194–200.
7. Takai Y, Ishiko S, Kagokawa H, Fukui K, Takahashi A, Yoshida A. Morphological study of acute zonal occult outer retinopathy (AZOOR) by multiplanar optical coherence tomography. Acta Ophthalmol. 2009;87:408–18.
8. Zibrandtsen N, Munch IC, Klemp K, Jørgensen TM, Sander B, Larsen M. Photoreceptor atrophy in acute zonal occult outer retinopathy. Acta Ophthalmol. 2008;86:913–6.
9. Spaide RF, Koizumi H, Freund KB. Photoreceptor outer segment abnormalities as a cause of blind spot enlargement in acute zonal occult outer retinopathy-complex diseases. Am J Ophthalmol. 2008;146:111–20.
10. Monson DM, Smith JR. Acute zonal occult outer retinopathy. Surv Ophthalmol. 2011;56:23–35.
11. So K, Shinoda K, Matsumoto CS, Satofuka S, Imamura Y, Mizota A. Focal functional and microstructural changes of photoreceptors in eyes with acute zonal occult outer retinopathy. Case Rep Ophthalmol. 2011;2:307–13.
12. Tsunoda K, Fujinami K, Miyake Y. Selective abnormality of cone outer segment tip line in acute zonal occult outer retinopathy as observed by spectral-domain optical coherence tomography. Arch Ophthalmol. 2011;129:1099–101.
13. Merino D, Duncan JL, Tiruveedhula P, Roorda A. Observation of cone and rod photoreceptors in normal subjects and patients using a new generation adaptive optics scanning laser ophthalmoscope. Biomed Opt Express. 2011;2:2189–201.
14. Mkrtchyan M, Lujan BJ, Merino D, Thirkill CE, Roorda A, Duncan JL. Outer retinal structure in patients with acute zonal occult outer retinopathy. Am J Ophthalmol. 2012;153:757–68.
15. Mahajan VB, Stone EM. Patients with an acute zonal occult outer retinopathy-like illness rapidly improve with valacyclovir treatment. Am J Ophthalmol. 2010;150:511–8.
16. Kitakawa T, Hayashi T, Takashina H, Mitooka K, Gekka T, Tsuneoka H. Improvement of central visual function following steroid pulse therapy in acute zonal occult outer retinopathy. Doc Ophthalmol. 2012;124:249–54.
17. Fletcher WA, Imes RK, Goodman D, Hoyt WF. Acute idiopathic blind spot enlargement. A big blind spot syndrome without optic disk edema. Arch Ophthalmol. 1988;106:44–9.
18. Watzke RC, Shults WT. Clinical features and natural history of the acute idiopathic enlargement blind spot syndrome. Ophthalmology. 2002;109:1326–35.
19. Gass JD. Are acute zonal occult outer retinopathy and the white spot syndromes (AZOOR complex) specific autoimmune diseases? Am J Ophthalmol. 2003;135:380–1.
20. Li D, Kishi S. Restored photoreceptor outer segment damage in multiple evanescent white dot syndrome. Ophthalmology. 2009;116:762–70.
21. Sloan LL. The threshold gradients of the rods and the cones: in the dark-adapted and in the partially light-adapted eye. Am J Ophthalmol. 1950;33:1077–89.
22. Elenius V. Rod saturation perimetry. Testing of the cone function with achromatic objects. Arch Ophthalmol. 1985;103:519–23.
23. Jacobson SG, Voigt WJ, Parel JM, Apáthy PP, Nghiem-Phu L, Myers SW, et al. Automated light- and dark-adapted perimetry for evaluating retinitis pigmentosa. Ophthalmology. 1986;93:1604–11.
24. Rotenstreich Y, Fishman GA, Lindeman M, Alexander KR. The application of chromatic dark-adapted kinetic perimetry to retinal diseases. Ophthalmology. 2004;111:1222–7.
25. Jacobson SG, Borruat FX, Apathy PP. Rod or cone dysfunction: uniocular presentations. Doc Ophthalmol. 1986;63:63–71.